Selective Electroless Copper Deposition by Using Photolithographic Polymer/Ag Nanocomposite

Ryspayeva, Assel; Jones, Thomas D. A.; Esfahani, Mohammadreza Nekouie; Shuttleworth, Matthew P.; Harris, Russell A.; Kay, Robert W.; Desmulliez, Marc P. Y.; Marques-hueso, Jose

DOI:
10.1109/TED.2019.2897258

Publication date:
2019

Document Version
Publisher's PDF, also known as Version of record

Selective Electroless Copper Deposition by Using Photolithographic Polymer/Ag Nanocomposite

Assel Ryspayeva, Thomas D. A. Jones, Mohammadreza Nekouie Esfahani, Matthew P. Shuttleworth, Russell A. Harris, Robert W. Kay, Marc P. Y. Desmulliez, *Senior Member, IEEE*, and Jose Marques-Hueso

***Abstract*— This paper presents a novel, direct, selective, vacuum-free, and low-cost method of electroless copper deposition, allowing additive patterning of nonconductive surfaces. Ag nanoparticles (NPs) synthesized inside a photosensitive polymer are acting as seeds for electroless copper deposition. The resulting copper film surface morphology was studied with scanning electron microscopy. Copper films were shown to display a rough grainlike structure, covering substrate uniformly with good metal-substrate adhesion. Copper thickness was studied as a function of the plating time, temperature, and Ag NPs seed concentration. A maximal copper thickness of 0.44 $\pm$ 0.05 μm was achieved when plated at 30 °C with 0.4 M Ag(I). The minimum feature resolution of copper patterns, grown with 0.025- and 0.1-M silver salt, is attained down to 10 μm. The maximum electrical conductivity of the copper film prepared with 0.025-, 0.1-, and 0.4-M Ag(I) approaches $(0.8 \pm 0.1) \times 10^7$ S/m, $(1.1 \pm 0.1) \times 10^7$ S/m and $(1.6 \pm 0.4) \times 10^7$ S/m, respectively. Electroless copper interconnections and LED circuit on glass substrate were fabricated as a proof of concept demonstrators.**

***Index Terms*— Ag nanoparticles (NPs) seeds, electroless copper, metallization of nonconductive surfaces, polymer/Ag nanocomposite.**

I. Introduction

ELECTROLESS metal deposition is a facile method to fabricate metallic patterns on nonconductive substrates. Electroless plating of sensor electrodes and interconnects in microtechnology and nanotechnology, such as functional printing, flexible electronics, wearable electronics, and the "Internet of Things," can reduce production cost as compared to other traditional metallization techniques [1]. Conventional track formation is a multistep photolithographic method producing conductive patterns by the removal of unwanted metal parts through etching processes. This pattern transfer method thus generates large quantities of waste. An alternative method is to deposit the metal by sputtering or evaporation. However, this process involves costly equipment and complex processing that consume high power to deposit metal layers. Moreover, vacuum requirements in processing increase the cost of the conventional metal patterning. Inkjet printing is another technique for printing conductive patterns on a substrate [2]. However, inkjet printing suffers from low manufacturing capability, while photolithography remains a dominant mass production method in the microelectronics industry [3]–[5]. Hence, there is continuous research in conductive track formation. Attempts have been made in metal patterning by using a combination of photolithography and electroless plating [6]. To fabricate metal patterns on nonconductive surfaces, a continuous seed layer is required [7]. The seed layer could be fabricated using a photolithographic approach, where metal NPs are synthesized inside a photosensitive polymer matrix, as reported by Marques-Hueso *et al.* [8], [9]. Metal NPs embedded inside the polymer can be used for further processing, such as nanostructure precursors [10], and it is viable that they could act as seeding sites for metal ions adsorption and continuous electrode formation.

Ag has successfully been used as a metal catalyst for electroless copper plating (ECP) [6]. Pd is a choice catalytic material for electroless plating due to its high activity [11]; however, palladium price per gram exceeds silver price by almost 70 times, limiting its use for large-scale production.

In this paper, we propose to fabricate copper microfeatures by ECP on the patterns formed by photolithography, using more economic Ag NPs as catalysts, as shown in Fig. 1. We demonstrate the formation of conductive copper tracks through the use of 2-diazo-2H-naphthalen-1-one (DNQ)-novolac polymer/Ag (hereafter—polymer/Ag) nanocomposite positive pattern on glass and silicon surfaces by photolithography, and its conversion to a copper pattern via electroless

Manuscript received October 17, 2018; revised December 31, 2018 and January 21, 2019; accepted January 29, 2019. This work was supported by the Engineering and Physical Sciences Research Council through Photobioform II under Grant EP/N018222/1 and Grant EP/N018265/2. The review of this paper was arranged by Editor M. S. Bakir. *(Corresponding author: Jose Marques-Hueso.)*

A. Ryspayeva, M. P. Y. Desmulliez, and J. Marques-Hueso are with the School of Engineering and Physical Sciences, Nature Inspired Manufacturing Centre, Heriot-Watt University, Edinburgh EH14 4AS, U.K. (e-mail: ra8@hw.ac.uk; m.desmulliez@hw.ac.uk; j.marques@hw.ac.uk).

T. D. A. Jones was with the School of Engineering and Physical Sciences, Nature Inspired Manufacturing Centre, Heriot-Watt University, Edinburgh EH14 4AS, U.K. He is now with the School of Science and Engineering, The University of Dundee, Dundee DD1 4HN, U.K. (e-mail: t.d.a.jones@dundee.ac.uk).

M. N. Esfahani, M. P. Shuttleworth, R. A. Harris, and R. W. Kay are with the Future Manufacturing Processes Research Group, School of Mechanical Engineering, University of Leeds, Leeds LS2 9JT, U.K. (e-mail: m.nekouieesfahani@leeds.ac.uk; mnmsh@leeds.ac.uk; r.harris@leeds.ac.uk; r.w.kay@leeds.ac.uk).

Color versions of one or more of the figures in this paper are available online at http://ieeexplore.ieee.org.

Digital Object Identifier 10.1109/TED.2019.2897258

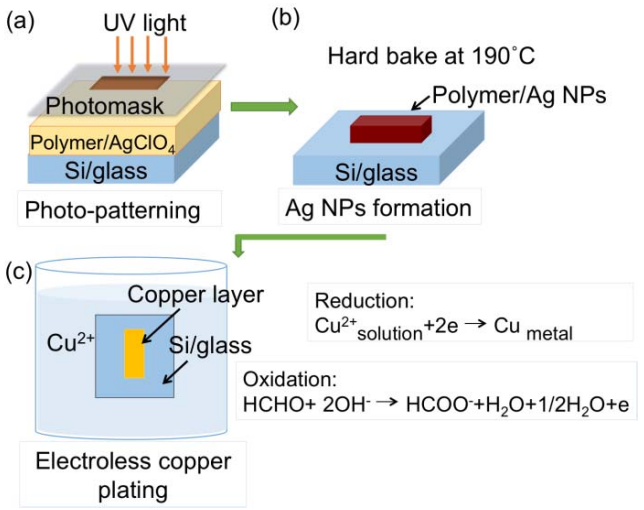

Fig. 1. Process steps for photopatterning and selective Cu deposition on silicon and glass substrates using (a) photolithography, (b) Ag NPs synthesis inside the polymer, and (c) direct deposition of Cu by electroless plating.

plating. This method benefits from not requiring vacuum, Ar and N_2 gaseous environments, and expensive equipment. The lithographic properties of the polymer allow direct photopatterning of metal tracks and interconnect on a desired substrate. The effect of the production parameters, such as plating temperature, plating time, and Ag NPs concentration, is discussed in this paper with a particular attention to copper film thickness, quality, feature resolution, and adhesion. Furthermore, adhesion of the copper film to a substrate and its effect on the copper film conductivity is also studied. Resilient interconnections between metal pads are demonstrated by the developed ECP method.

II. Experiments

A. Materials

This paper used the following materials. Silver perchlorate (Sigma Aldrich, 97%), 1-methoxy 2-propylacetate (MPA) (Sigma Aldrich, 99%), DNQ-novolac positive tone photoresist (Ma-P 1215, Microresist Technology), AZ 326 developer (Microresist Technology), copper sulfate (98%, Sigma Aldrich), sodium hydroxide (98.5%, Acros Organics) potassium tartrate (99%, Fisher Scientific), and formaldehyde (37%, Acros Organics).

B. Synthesis of Ag NPs Seed Layer

0.025-, 0.1-, and 0.4-M silver perchlorate ($AgClO_4$) concentrations were prepared by direct dissolution in MPA. DNQ-novolac photosensitive polymer (hereafter—polymer) was mixed with the silver solution in 1:1 ratio. The resultant mixture was spin coated on silicon and glass substrates at 3000 r/min for 30 s and soft baked at 45 °C for 10 min. Silicon (15 mm × 15 mm) and glass (18 mm × 18 mm) substrates were exposed to UV light at 14 $mW \cdot cm^{-2}$ in Karl Suss MJB 3 UV mask aligner and developed with AZ 326 developer diluted with deionized water (DI) in 1:1 ratio. The samples were hard baked at 190 °C for 10 min on a hot plate leading to the thermal reduction of Ag(I) to Ag NPs inside the polymer.

C. Fabrication of Electroless Copper Films and Interconnections

Electroless copper bath solution was prepared using the formulation in [12] by dissolving 6 g of copper sulfate, 8 g of sodium hydroxide, and 28 g of potassium tartrate into 200 ml of DI water. Before electroless plating, the concentrated solution was diluted with DI water in the ratio of 1:1 and 2 ml of formaldehyde was added. Treated substrates were immersed into electroless copper bath for the allocated time. Electroless plating was conducted at room temperature (RT) and 30 °C.

Metal pads were fabricated as a testing environment to study electroless copper interconnection behavior. Test metal pads consisted of 200-nm copper on 50-nm Ti and were fabricated by UV-lithography, e-beam thermal evaporation, and liftoff process. The sizes of the fabricated test metal pads are 300 μm × 300 μm and 500 μm × 500 μm.

D. Characterizations

The presence of Ag NPs and their optical and structural properties were characterized by a UV-2550 spectrophotometer. Copper film thickness was measured by Dektak[3] Stylus optical profilometer. To obtain the copper thickness for each configuration, three samples were prepared and average copper thicknesses with corresponding standard deviations were calculated. Optical images of the film surface were obtained using a LEICA CTR 6500 microscope. The surface morphology of copper film was studied with scanning electron microscopy (SEM) Quanta 650 field emission gun.

The conductivity of the copper films was obtained by four-point probe using the van der Pauw technique [13]. To acquire copper conductivity for each configuration, three samples were prepared and average copper conductivity with corresponding standard deviations was calculated for each of the samples. Square glass substrates (22 mm × 22 mm) were used for copper layer deposition. The van der Pauw method involves the application of a current (I), and the measurement of the resulting voltage (V) using four small contacts on the perimeter of the sample. Therefore, four probes were attached at the edges of the square sample. Four measurement configurations at each probe location for forward and reverse current were performed, and conductivity was found as an inverse of the resistivity, where resistivity, ρ, was calculated as [14], [15]

$$\rho = \frac{\pi}{\ln(2)} t \frac{(R_a + R_b)}{2} F \tag{1}$$

where t is a copper thickness, F is a correction factor, and R_a and R_b are as follows:

$$R_a = \frac{\frac{V_{f34}}{I_{f21}} + \frac{V_{r34}}{I_{r21}} + \frac{V_{f12}}{I_{f43}} + \frac{V_{r12}}{I_{r43}}}{4} \tag{2}$$

$$R_b = \frac{\frac{V_{f41}}{I_{f32}} + \frac{V_{r41}}{I_{r32}} + \frac{V_{f23}}{I_{f14}} + \frac{V_{r23}}{I_{r14}}}{4}. \tag{3}$$

The subscripts f and r stand for forward and reverse current directions, respectively. For symmetrical samples, such as the square, $F = 1$ [14].

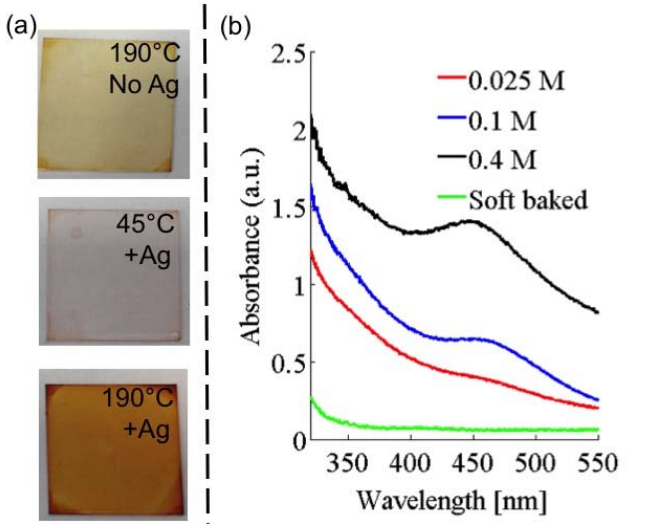

Fig. 2. (a) Images of glass substrates (see descriptions on the figure) and (b) UV-vis absorbance spectra of polymer/Ag nanocomposite prepared with 0.025-, 0.1-, and 0.4-M Ag(I) salt after samples were hard baked at 190 °C, and a reference sample acquired after a soft bake at 45 °C.

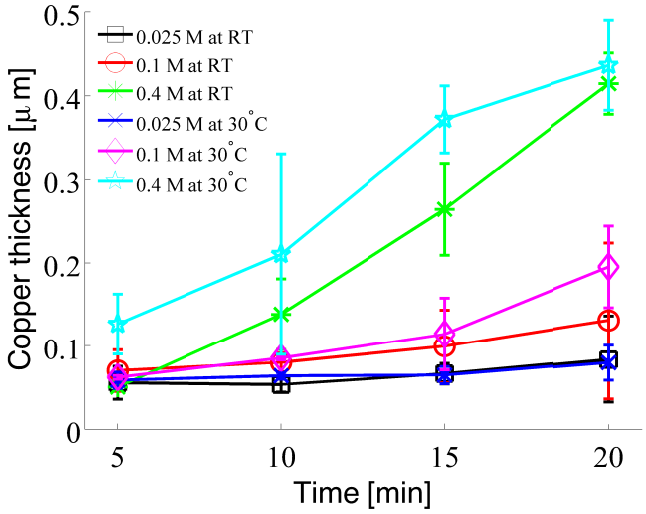

Fig. 3. Copper thickness as a function of $AgClO_4$ salt concentration, electroless plating time, and temperature.

Resistance of the tests pads with electroless copper interconnections was measured using two probes in the SIGNATONE S-1160 probe station. The diameter of the probe tips is 80 μm with the electrodes spaced at around 1 mm. Test metal pads of 500 μm $\times$ 500 μm sizes were used for resistance characterizations. Parasitic resistances were assumed to be negligible.

III. Results and Discussion

A. Ag NPs Seed Layer Characterization

Fig. 2(a) shows the appearance of polymer and polymer/Ag structures on glass substrates after a hard (190 °C) and soft (45 °C) bake. Polymer/Ag structure changes color from light yellow to dark brown when hard baked, indicating a formation of Ag NPs by thermal reduction [9]. Fig. 2(b) shows UV-vis absorbance spectra of the polymer/Ag nanocomposites after a hard and soft bake. Ag NPs display localized surface plasmon resonance (LSPR) occurring near 400–500 nm [16]. Therefore, LSPR maxima occurring here indicates the presence and formation of Ag NPs during a hard bake for the three Ag(I) salt concentrations. Single and broad LSPR peak indicates that Ag NPs have spherical shapes with a broad size distribution and sizes up to 100 nm [17]. LSPR intensity rises with higher Ag(I) salt concentrations, which implies that the amount of Ag NPs embedded inside the polymer increases [18].

B. Effect of Plating Time, Temperature, and Ag NPs Concentration on the Copper Film

Fig. 3 displays a plot of the plated copper thicknesses on the silicon substrate as a function of plating time. Copper thickness grows linearly with plating time which is in agreement with the previously published work [19], [20]. A maximal copper thickness of 0.44 $\pm$ 0.05 μm was achieved when plated at 30 °C with 0.4-M Ag(I) and an increase to Ag NPs concentration also produced thicker copper layers. This may be due to densely packed Ag NPs in the polymer, which created more sites for copper ion adsorption at the higher temperatures and concentrations.

The effect of the plating temperature on the copper surface morphology is shown in Fig. 4(a)–(c). SEM micrographs taken after 10 min of ECP show that the copper film has a rough granular structure covering the polymer surface uniformly, when plated both at RT and at 30 °C. However, the surface of the copper film deposited at RT has voids between the copper grains and appears more porous compared to the copper film plated at 30 °C, as observed in [21]. Therefore, plating at 30 °C produces thicker copper layers and a more uniform and continuous copper film.

C. Effect of Ag NPs Concentration on Film Ductility

Fabricated copper films are free of cracks and defects; however, electroless copper films frequently suffer from poor ductility due to buildup of internal stress, which was also observed in [22] and [23]. In the present technique, delamination of copper film may occur after plating time reaches a certain threshold. Fig. 4(d) and (e) shows the visual appearance of the copper film prepared with varied Ag(I) salts concentrations. Copper film grown with 0.025-M Ag(I) displayed delamination at 8 min. SEM images in Fig. 4 show qualitatively that the copper film ductility improved with the increase in Ag(I) salt concentration. For example, copper obtained with 0.1- and 0.4-M Ag(I) only delaminated after 12 min. This copper peeling process can be understood by analyzing the copper growth mechanism. The growth of a copper thin film (up to 1 μm) undergoes three stages: nucleation, growth, and coalescence of three-dimensional crystallites (TDCs) [24]. Coalescence is the most important stage, in which crystal building process results in the formation of a continuous copper film. Therefore, copper cracks may occur due to the built-up stress and formation of voids between TDC. Also, since the reduction of both copper and hydrogen takes place simultaneously, the probability of incorporating H and H_2 into the copper deposition is high [25]. Hydrogen traps contribute

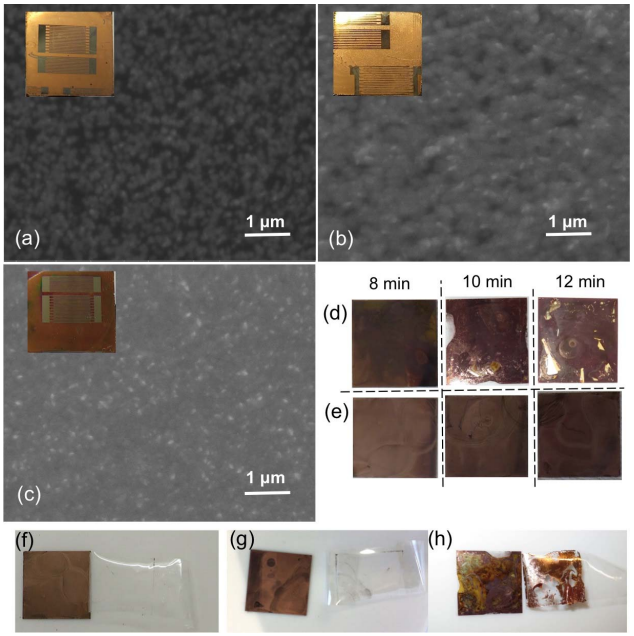

Fig. 4. SEM micrographs of the copper surface prepared with (a) 0.4-M Ag(I) and plated at RT for 10 min, (b) 0.4-M Ag(I) and plated at 30 °C for 10 min, and (c) 0.1-M Ag(I) and plated at 30 °C for 10 min. Insets: photographs of micropatterns on silicon substrates. Photographs of the copper films on the glass substrates plated at 30 °C for 12 min with Ag(I) concentrations of (d) 0.025 M and (e) 0.4 M. Photographs of the copper films on the glass substrates and corresponding tapes after a scotch-tape tests (f) 10-min ECP, 0.4-M Ag(I), (g) 10-min ECP, 0.1-M Ag(I), and (h) 10-min ECP, 0.025-M Ag(I).

to the formation of voids and may lead to a porous copper structure [26]. Therefore, Ag NP concentration should remain high to increase copper density and to eliminate void formation between the copper grains. Hence, seed layers with 0.1 and 0.4-M Ag(I) are more favorable to produce continuous copper films.

When applying the IPC-TM-650 scotch-tape tests [27] to copper films prepared at 0.4-M Ag(I) shown in Fig. 4(f), the adhesions of the copper films to glass substrates show a good strength, with no observable removal of the metal parts from the substrate. As for copper films prepared with 0.1-M Ag(I), minor removal of the copper was observed at the edges of the glass substrate [see Fig. 4(g)]. However, copper films prepared with a low-Ag NPs seed concentration [0.025-M Ag(I)] and plated beyond the plating time threshold, as shown in Fig. 4(h), display delamination due to scotch tape test.

D. Resolution and Selectivity

Fig. 5 shows optical images of copper patterns after photolithography and ECP with pitch sizes of 40 and 20 μm on silicon substrate. It is seen that copper plates uniformly on the surface of the polymer/Ag nanocomposite preserving the lithographic pattern. Copper films grown with 0.025- and 0.1-M silver salt present well-resolved features down to 10 μm. It was found that the lithographic performance of polymer is affected by the presence of Ag(I) salt, as the resolution is poorer for patterns prepared with 0.4-M silver salt. This could be due to the increased concentration of the embedded Ag NPs, leading to the poorer stripping performance of the polymer during the development step. Therefore, copper plating on the poorly developed sites affects the overall feature resolution. Fig. 6 shows optical images of the copper features with a fine resolution down to 10 μm. ECP shows a good selectivity allowing targeting and plating on specific localized areas. Therefore, this method demonstrates excellent selectivity where the copper plates uniformly only on the catalyzed surfaces.

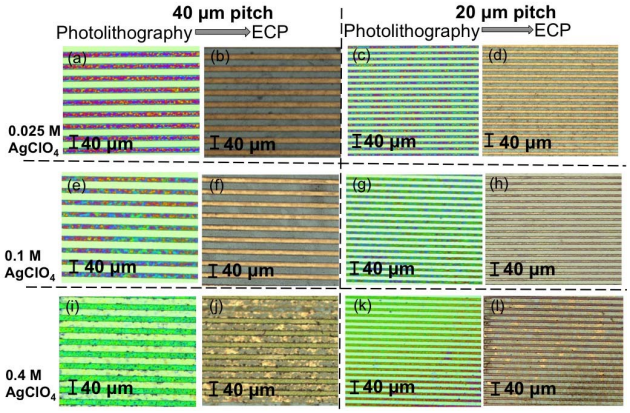

Fig. 5. Optical images of the patterns taken after photolithography and ECP, with Ag(I) concentrations of (a)–(d) 0.025 M, (e)–(h) 0.1 M, and (i)–(l) 0.4 M.

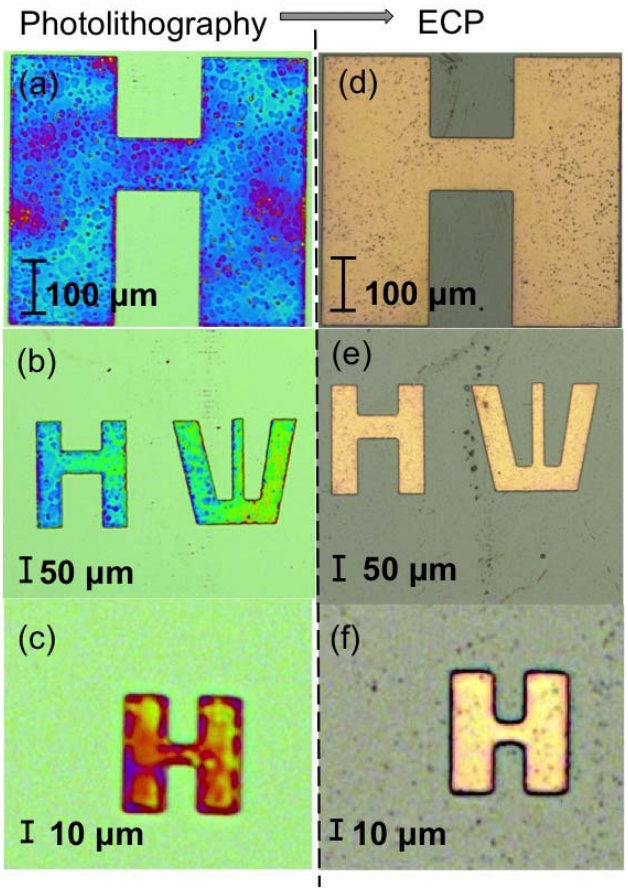

Fig. 6. Optical images of the patterns prepared with 0.025-M Ag(I). Images were taken after (a)–(c) photolithography and after (d)–(f) ECP steps.

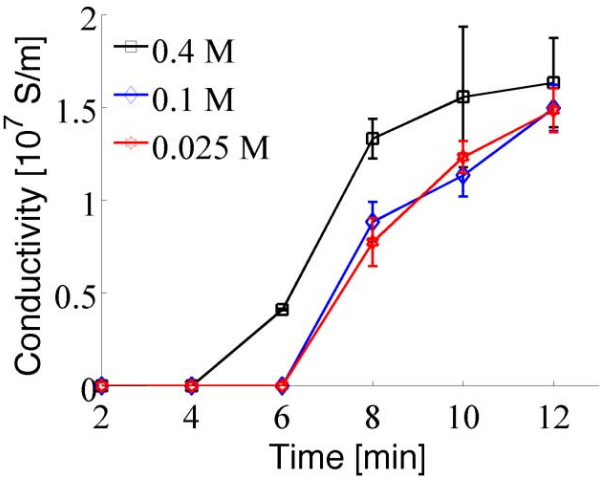

Fig. 7. Conductivity measurements at different plating times for 0.025-, 0.1-, and 0.4-M Ag(I) measured with four-point probe.

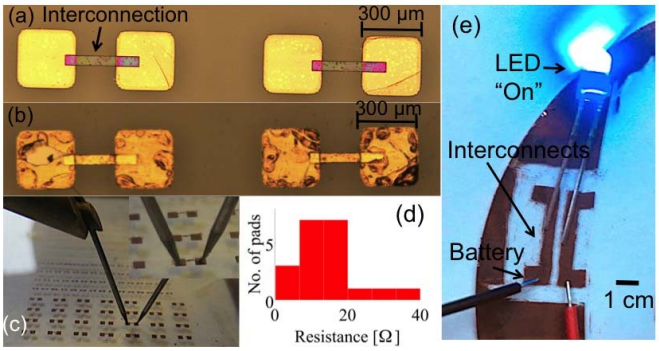

Fig. 8. (a) Images of the 300 μm × 300 μm pads with the electroless copper interconnections after photolithography and (b) after ECP. (c) Measurement of the resistance using two probes with the probes placed on 500 μm × 500 μm pads. Distance between the pads is 500 μm. Inset: a magnified image of the probe tips landing on the pads. (d) Distribution of the measured resistances per number of pads. (e) LED circuit connected to a 3-V battery.

E. Influence of the Copper Thickness on Conductivity

Fig. 7 shows the electroless copper conductivity as a function of plating time for several salt concentrations. Before any copper delamination occurs, the maximum electrical conductivity of the copper film prepared with 0.025-M Ag(I) approaches $(0.8 \pm 0.1) \times 10^7$ S/m at 8 min. For copper films prepared with 0.1- and 0.4-M Ag(I), the conductivity grows to $(1.1 \pm 0.1) \times 10^7$ S/m and $(1.6 \pm 0.4) \times 10^7$ S/m at 10 min, respectively. This is close to previously reported measurements on electroless copper conductivity [23], [28]. These values compare favorably to the electrical conductivity of bulk copper at 5.96×10^7 S/m.

There is, therefore, a tradeoff between the copper thickness and copper film conductivity. Copper films prepared with 0.1- and 0.4-M Ag(I) salts are promising for interconnection fabrication since they can provide thicker copper patterns with a good adherence to a substrate while still approaching the bulk copper conductivity.

F. Electroless Copper Interconnections

As a demonstration of the electroless interconnections between the rigid parts, Fig. 8(a) and (b) shows the optical images of the interconnections after photolithography and ECP. Electroless copper successfully interconnected test pads and plated on the top of the metal pads and polymer/Ag nanocomposite. The 0.1-M Ag(I) was used and the metal features were plated for 10 min. To demonstrate that electroless interconnects are able to link pads, the electrical resistance was measured. The average resistance was found as 14 ± 8 Ω. The resistance of the interconnections could be affected by the nonuniformity of the copper thicknesses of the formed interconnections (0.59 ± 0.06) μm and pads (0.87 ± 0.07) μm. The growth of the electroless copper depends on the catalytic activity of the seeds [29]. Evaporated copper consists of closely packed nanocrystallites, which are distributed uniformly on the substrate [30], [31]. Therefore, copper nanocrystallites act as seeds for electroless copper growth. A high coverage of the surface and a reduction in seed size provides a larger surface area enabling faster plating rates as there is less incorporation of hydrogen bubbles influencing copper ductility [29]. Therefore, the plating rates for electroless copper onto evaporated copper are faster than on the polymer/Ag nanocomposites, as Ag seeds in the polymer are rather widely distributed in the polymer matrix which makes the plating rate slower [29]. Therefore, electroless copper plated onto evaporated copper metal results in a thicker copper layer than plated onto polymer/Ag nanocomposite.

An LED circuit was constructed to further demonstrate the electroless copper metallization quality and electrical conductivity. Fig. 8(e) illustrates the functional LED circuit on a glass substrate prepared using a homemade photomask. The electroless copper interconnections were prepared with 0.1-M Ag(I) and plated for 10 min. The 3-mm LED was placed on the fabricated copper tracks and a 3-V battery was connected. When the battery was switched on, the LED turned on, which signifies that the prepared electroless copper has a good electrical conductivity.

IV. Conclusion

Uniform copper films with good electrical properties were obtained on silicon and glass substrates by a newly developed ECP method that minimizes processing steps. Ag NPs embedded inside the polymer successfully induced the activation of noncatalytic surfaces. It was found that the electroless copper thickness depends on the concentrations of the Ag NPs, plating temperature, and plating time. Copper films prepared with 0.1- and 0.4-M Ag(I) salts have stronger adhesion to the substrates than copper films prepared with 0.025-M Ag(I). The minimum fabricated feature size is 10μm, which is the best resolution obtained with 0.025- and 0.1-M Ag(I). The conductivity of the fabricated electroless copper films is in the range of bulk copper conductivity. The method has been demonstrated to be suited for cost-effective metallization for conductive track formation.

ACKNOWLEDGMENT

The authors would like to thank the staff members at Heriot-Watt University, N. Ross and M. Leonard for their assistance with the microfabrication facilities and Dr. N. Bennett, Dr. P. Szabo, and E. Acosta for providing access to electrical characterization facilities.

REFERENCES

[1] Y. Shacham-Diamand, T. Osaka, Y. Okinaka, A. Sugiyama, and V. Dubin, "30 years of electroless plating for semiconductor and polymer micro-systems," *Microelectron. Eng.*, vol. 132, pp. 35–45, Jan. 2015.

[2] S. Khan, L. Lorenzelli, and R. S. Dahiya, "Technologies for printing sensors and electronics over large flexible substrates: A review," *IEEE Sensors J.*, vol. 15, no. 6, pp. 3164–3185, Jun. 2015.

[3] E. Buitrago, T. S. Kulmala, R. Fallica, and Y. Ekinci, "EUV lithography process challenges," in *Frontiers Nanosci.*, vol. 11, pp. 135–176, 2016.

[4] Y. Liu, J. Genzer, and M. D. Dickey, "'2D or not 2D': Shape-programming polymer sheets," *Prog. Polym. Sci.*, vol. 52, pp. 79–106, Jan. 2016.

[5] H. Bikas, P. Stavropoulos, and G. Chryssolouris, "Additive manufacturing methods and modelling approaches: A critical review," *Int. J. Adv. Manuf. Technol.*, vol. 83, nos. 1–4, pp. 389–405, 2016.

[6] R. Abargues, M. L. Martinez-Marco, P. J. Rodriguez-Canto, J. Marques-Hueso, and J. Martinez-Pastor, "Metal-polymer nanocomposite resist: a step towards *in-situ* nanopatterns metallization," *Proc. SPIE*, vol. 8682, Mar. 2013, Art. no. 86820X.

[7] J. Marques-Hueso *et al.*, "A rapid photopatterning method for selective plating of 2D and 3D microcircuitry on polyetherimide," *Adv. Funct. Mater.*, vol. 28, no. 6, 2018, Art. no. 1704451.

[8] J. Marques-Hueso, R. Abargues, J. Canet-Ferrer, J. L. Valdes, and J. Martinez-Pastor, "Resist-based silver nanocomposites synthesized by lithographic methods," *Microelectron. Eng.*, vol. 87, nos. 5–8, pp. 1147–1149, 2010.

[9] J. Marqués-Hueso, R. Abargues, J. L. Valdés, and J. P. Martínez-Pastor, "Ag and Au/DNQ-novolac nanocomposites patternable by ultraviolet lithography: A fast route to plasmonic sensor microfabrication," *J. Mater. Chem.*, vol. 20, no. 35, pp. 7436–7443, 2010.

[10] J. Marqués-Hueso, J. A. S. Morton, X. Wang, E. Bertran-Serra, and M. P. Y. Desmulliez, "Photolithographic nanoseeding method for selective synthesis of metal-catalysed nanostructures," *Nanotechnology*, vol. 30, no. 1, 2018, Art. no. 015302.

[11] T. Tamai, M. Watanabe, S. Watase, N. Nishioka, and K. Matsukawa, "Direct electroless copper deposition on a photolithographic pattern of palladium-nanoparticle/acrylic-polymer hybrid," *Trans. Jpn. Inst. Electron. Packag.*, vol. 4, no. 1, pp. 110–113, 2011.

[12] R. A. Farrer *et al.*, "Selective functionalization of 3-D polymer microstructures," *J. Amer. Chem. Soc.*, vol. 128, no. 6, pp. 1796–1797, 2006.

[13] L. J. van der Pauw, "A method of measuring the resistivity and Hall coefficient on lamellae of arbitrary shape," *Philips Tech. Rev.*, vol. 20, pp. 220–224, 1958.

[14] D. K. Schroder, *Semiconductor Material and Device Characterization*, vol. 44, no. 4, 3rd ed. Hoboken, NJ, USA: Wiley, 2006.

[15] M. P. Gutiérrez, L. Haiyong, and J. Patton, *Thin Film Surface Resistivity*. 2002.

[16] R. Abargues *et al.*, "Optical properties of different polymer thin films containing *in situ* synthesized Ag and Au nanoparticles," *New J. Chem.*, vol. 33, no. 8, pp. 1720–1725, 2009.

[17] M. A. Raza, Z. Kanwal, A. Rauf, A. N. Sabri, S. Riaz, and S. Naseem, "Size-and shape-dependent antibacterial studies of silver nanoparticles synthesized by wet chemical routes," *Nanomaterials*, vol. 6, no. 4, p. 74, 2016.

[18] D. dos Santos Courrol *et al.*, "Optical properties and antimicrobial effects of silver nanoparticles synthesized by femtosecond laser photoreduction," *Opt. Laser Technol.*, vol. 103, pp. 233–238, Jul. 2018.

[19] A. Kaewvilai, R. Tanathakorn, A. Laobuthee, W. Rattanasakulthong, and A. Rodchanarowan, "Electroless copper plating on nano-silver activated glass substrate: A single-step activation," *Surf. Coat. Technol.*, vol. 319, pp. 260–266, Jun. 2017.

[20] S. Ma, L. Liu, V. Bromberg, and T. J. Singler, "Electroless copper plating of inkjet-printed polydopamine nanoparticles: A facile method to fabricate highly conductive patterns at near room temperature," *ACS Appl. Mater. Interfaces*, vol. 6, no. 22, pp. 19494–19498, 2014.

[21] Y. Lantasov, R. Palmans, and K. Maex, "New plating bath for electroless copper deposition on sputtered barrier layers," *Microelectron. Eng.*, vol. 50, nos. 1–4, pp. 441–447, Jan. 2000.

[22] J. F. Rohan, G. O'Riordan, and J. Boardman, "Selective electroless nickel deposition on copper as a final barrier/bonding layer material for microelectronics applications," *Appl. Surf. Sci.*, vol. 185, nos. 3–4, pp. 289–297, 2002.

[23] R. K. Aithal, S. Yenamandra, R. A. Gunasekaran, P. Coane, and K. Varahramyan, "Electroless copper deposition on silicon with titanium seed layer," *Mater. Chem. Phys.*, vol. 98, no. 1, pp. 95–102, 2006.

[24] M. Paunovic, "Electroless deposition of copper," in *Modern Electroplating*, vol. 1. 2010, pp. 433–446.

[25] S. Nakahara and Y. Okinaka, "The hydrogen effect in copper," *Mater. Sci. Eng., A*, vol. 101, pp. 227–230, May 1988.

[26] S. Nakahara, "Microscopic mechanism of the hydrogen effect on the ductility of electroless copper," *Acta Metallurgica*, vol. 36, no. 7, pp. 1669–1681, Jul. 1988.

[27] *IPC TM-650 Test Methods Manual*, Sanders Road Northbrook, IL, USA, 2004.

[28] C.-Y. Kao and K.-S. Chou, "Electroless copper plating onto printed lines of nanosized silver seeds," *Electrochem. Solid-State Lett.*, vol. 10, no. 3, pp. D32–D34, 2007.

[29] T. D. A. Jones *et al.*, "Direct metallisation of polyetherimide substrates by activation with different metals," *Surf. Coat. Technol.*, vol. 360, pp. 285–296, Feb. 2019.

[30] H. Komalakrishna, A. Augustin, and K. U. Bhat, "Electron beam deposition of copper thin film on aluminium substrate and its characterization," *Amer. J. Mater. Sci.*, vol. 5, no. 3C, pp. 19–24, 2015.

[31] Y. H. Navale *et al.*, "Thermally evaporated copper oxide films: A view of annealing effect on physical and gas sensing properties," *Ceram. Int.*, vol. 43, no. 9, pp. 7057–7064, Jun. 2017.